

Exchange-correlation potential for inhomogeneous electron systems at finite temperatures

Uday Gupta and A. K. Rajagopal

Department of Physics and Astronomy, Louisiana State University, Baton Rouge, Louisiana 70803

(Received 28 April 1980)

The basis for a density-functional theory of inhomogeneous electron systems at finite temperatures is a suitable exchange-correlation potential. A local potential is presented here for a wide range of densities and temperatures based on the first-order exchange and sum of ring diagrams for the interacting homogeneous electron gas. The validity of this scheme in the different temperature-density regions is discussed. It is found that the correlations dominate over the first-order exchange contributions over a wide range of temperatures for a given density.

I. INTRODUCTION

A description of systems in thermodynamic equilibrium can be given in terms of a Schrödinger-type equation with an effective self-consistent potential V_{xc} , due to the mutual interactions of the particles of the system appearing in it as a basic input. This is a development parallel to the description of the ground-state properties of such systems at zero temperature. For a review of the basic formalism due to Hohenberg, Kohn, Sham, and Mermin and a large variety of applications of the zero-temperature formalism and many references to the original works, one may refer to the recent review article of Rajagopal.¹ The finite-temperature theory is not in the same state as the zero-temperature theory partly because the appropriate potential has not yet been set up. The work of Rozsnyai² examines atomic properties at high temperatures and pressures. He uses a local potential which interpolates between the known high-density zero-temperature and the low-density high-temperature answers. McMahan and Ross³ study the high-temperature electron-band structures in an effort to understand shock compression data, and employ a zero temperature, local V_{xc} because the data examined corresponded essentially to a low-temperature high-density regime. In these calculations, the dependence on temperature is brought in only via the appropriate definition of local density. Recently we⁴ presented a local potential containing only the lowest-order exchange processes for all temperatures. Such a potential provides the finite-temperature generalization of the exchange-only approximation of the zero-temperature theory.¹ Since the correlation contributions are expected to persist for temperatures where the exchange contribution has become vanishingly small, it is important to examine the nature of these contributions in some scheme. Since no V_{xc} for finite temperatures is known to exist in the literature, we believe the present work fills a gap in this area of considerable interest.

It may not be out of place here to spell out the parameters that enter in a theoretical discussion of the temperature-dependent properties of an interacting electron gas. There are two parameters in the problem, namely, the density n and the temperature T of the system. In the limit of no interaction among the electrons, the degeneracy parameter which is the ratio of the chemical potential to the thermal energy ($k_B T$) suffices to describe the system for all regions of density and temperature. When the interaction among the electrons is taken into account, this simplicity is lost and we need to specify the two variables n and T . In the lowest order of perturbation calculation of the contributions due to interaction, we have the well-known Hartree-Fock (HF) result and here the results depend on n and T as a product of a function of n alone and another function of the degeneracy parameter.⁴ When we go beyond the HF scheme, we find even this simplified parametrization is lost and we need to specify both n and T .

These features may be physically understood by realizing the fact that there are three basic lengths in this system, namely, the Bohr radius coming from the intrinsic interactions among the electrons, the inverse of the Fermi momentum (k_F) arising from the fact that we have a many electron system of a given density, and finally the deBroglie wavelength λ_T , associated with the temperature of the system. Out of these, basically two dimensionless parameters may be used to describe our system. For, example, the ratio of the Fermi wavelength to the Bohr radius ($k_F a_0$) used to describe the zero-temperature interacting electron system and the ratio of λ_T to the inverse Fermi momentum ($k_F \lambda_T$) for describing the temperature effects in a system of a given density. The latter, it turns out, is related to the ratio of the Fermi temperature to the temperature of the system. Thus we observe that in the noninteracting system, the theory involves only the latter parameter for all n and T because the degeneracy parameter becomes a unique function of this, and as we include the interactions, the two dimensionless

parameters both enter the theoretical description of our system. We may also point out that any other parametrization, such as plasma parameter, etc., are all expressible in terms of those we introduced above. We thus note that in our description of the system, we employ n and T directly, as this seems to be the most direct way of parametrizing our results, as well as the most appropriate ones in a density functional formalism.

As in the zero-temperature case, we propose to employ the properties of the homogeneous electron gas as the source for generating the starting potential V_{xc} . We present here V_{xc} for a wide range of temperatures and densities by an actual numerical evaluation of the discrete "frequency" series arising from the sum of "ring" diagrams for the exchange-correlation part of the grand potential Ω_{xc} of the electron gas. We give below the reasons for this choice and also discuss the regions of validity of the scheme.

Broadly speaking, we have four regions: (1) low temperature, low density; (2) low temperature, high density; (3) high temperature, low density; and (4) high temperature, high density. In (1), a perturbation approach is invalid because the system prefers to be in an ordered crystalline state and so this region is outside the scope of the ring diagrams. In (2), some exact answers are known. At zero temperature, Gell-Mann and Brueckner⁵ showed that in the limit of very high densities, the sum of ring diagrams gives the exact answer, being the most divergent set of diagrams. In the extreme low-density limit at zero temperature, on the other hand, Iwata⁶ showed that the same set of ring diagrams reproduce the two lowest-order terms of Nozières and Pines.⁷ It is now common knowledge that the correlation energy at intermediate densities obtained from these ring diagrams is quite reasonable and, in fact, the most commonly used expression for V_{xc} at $T=0$ K is that due to von Barth and Hedin⁸ which is based on the numerical evaluation of the sum of ring diagram contributions. It was Montroll and Ward⁹ who obtained the free energy of the electron gas for nonzero T in terms of a diagrammatic perturbation series. In particular, they formally summed a class of ring diagrams which in the zero-temperature limit is the same as the set of diagrams considered by Gell-Mann and Brueckner. Here again, these diagrams form the most divergent set. In region (3), exact results are known and, in fact, DeWitt¹⁰ showed that for low densities and in the $T \rightarrow \infty$ limit, one may replace the Fermi-Dirac distribution by a Maxwell-Boltzmann distribution and deduce from these the classical Debye-Hückel result for the correlation contri-

bution to the free energy. This result is widely used in the calculation of the thermodynamic properties of high-temperature plasmas. Kraeft *et al.*¹¹ have evaluated the sum of the ring diagrams for the correlation part of the free energy, denoted by $\Omega_c^{(r)}$ in ranges of temperatures and densities appropriate to gaseous and solid state plasmas by retaining the Fermi-Dirac distribution. Given the success of the ring sum to give a fair account of regions (2) and (3), we expect that it may be an adequate approximation for our purposes in region (4). In the present paper, we have evaluated $\Omega_c^{(r)}$ as well as $V_c^{(r)}$ the correlation part of the effective potential due to ring diagrams for a wide range of temperatures and densities.

In the second section, a brief outline of the ring diagram sum for the grand potential is given. From this, we deduce an expression for $V_c^{(r)}$. In the third section, the numerical results are given and they are discussed in the light of known answers in regions (2) and (3). In the final section, a summary of the results is given.

II. A BRIEF THEORETICAL ACCOUNT

For a homogeneous, interacting electron system in thermal equilibrium at a temperature T , the thermodynamic potential Ω in the grand canonical ensemble is given by¹²

$$\Omega(T, V_0, \mu) = \Omega_0(T, V_0, \mu) + \Omega_{xc}(T, V_0, \mu), \quad (1)$$

where Ω_0 is the corresponding quantity for the noninteracting system at a temperature T confined to a volume V_0 with a chemical potential μ . Ω_{xc} is the exchange and correlation contributions to the thermodynamic potential. We use units and notations as in Ref. 4. In the lowest order of perturbation theory in the Coulomb interaction between the electrons, we obtain the exchange part, Ω_x :

$$\Omega_x = -V_0 \int \int \frac{d^3k d^3q}{(2\pi)^6} V(\vec{k} - \vec{q}) f(k) f(q). \quad (2)$$

The sum of ring diagrams leads to the correlation part $\Omega_c^{(r)}$ given by¹²

$$\Omega_c^{(r)} = \frac{V_0}{2\beta} \sum_{i=-\infty}^{\infty} \int \frac{d^3q}{(2\pi)^3} \{ \ln[1 - V(q)\chi(q, \nu_i)] + V(q)\chi(q, \nu_i) \}, \quad (3)$$

where $\chi(\vec{q}, \nu_i)$ is the "polarization" due to the density fluctuation in the system given by

$$\chi(\vec{q}, \nu_i) = -2 \int \frac{d^3p}{(2\pi)^3} \frac{f(\vec{p} + \vec{q}) - f(\vec{p})}{i\nu_i \hbar - \frac{\hbar^2}{2m} (|\vec{p} + \vec{q}|^2 - p^2)}, \quad (4)$$

where

$$\nu_i = \frac{2i\pi}{\beta \hbar}.$$

To obtain the exchange-correlation potential $V_{xc}[n, T]$, we need to evaluate the functional derivation of Ω_{xc} with respect to the density $n(=N/V_0)$ of the system. In the scheme outlined above, Ω_{xc} is a sum of Ω_x and $\Omega_c^{(r)}$ as a consequence of the

perturbation scheme. As in Ref. 4, scaling all the variable appropriately, ($t=T/T_F$), we obtain

$$V_{xc}[n, T] = V_x[n, T] + V_c^{(r)}[n, T], \quad (5)$$

where

$$V_x[n, T] = -\frac{e^2}{\pi} (3\pi^2 n)^{1/3} \frac{1}{\int_0^\infty dx x^2 f(x)[1-f(x)]} \int_0^\infty \int_0^\infty dx dy x f(x) y f(y) [1-f(y)] \ln \left| \frac{x+y}{x-y} \right|, \quad (6)$$

and

$$V_c^{(r)}[n, T] = \frac{e^2}{4\pi} (3\pi^2 n)^{1/3} t \frac{1}{\int_0^\infty dx x^2 f(x)[1-f(x)]} \sum_{l=-\infty}^{\infty} \int_0^\infty dQ \frac{V(Q) \chi(Q, \nu_l)}{1 - V(Q) \chi(Q, \nu_l)} \frac{1}{Q} \int_0^\infty dx x f(x) [1-f(x)] \times \ln \left(\frac{4l^2 \pi^2 t^2 + (Q^2 + 2Qx)^2}{4l^2 \pi^2 t^2 + (Q^2 - 2Qx)^2} \right), \quad (7)$$

where

$$V(Q) \chi(Q, \nu_l) = -\frac{2}{\pi a_0 k_F Q^3} \int_0^\infty dx x f(x) \ln \left(\frac{4l^2 \pi^2 t^2 + (Q^2 + 2Qx)^2}{4l^2 \pi^2 t^2 + (Q^2 - 2Qx)^2} \right). \quad (8)$$

In Ref. 4, $\Omega_x[n, T]$ and $V_x[n, T]$ were presented. It was found that $\Omega_x[n, T]/\Omega_x[n, 0]$ and $V_x[n, T]/V_x[n, 0]$ are functions of t only. This simplification does not occur for the correlation part. For every density, a range of t between 0 and 10 is found to be most interesting. We present the data for n ranging from $10^{18}/\text{cm}^3$ to $10^{26}/\text{cm}^3$ in this temperature region. The density range chosen is appropriate for atomic systems, laser plasmas, and solid state systems. We found that the summation of the l series has distinct advantages over an integral version which could be deduced from the sum forms by a contour integration trick. A discussion of these aspects is also given in the next section.

III. RESULTS

In Tables I(a)–I(d) we present Ω_x , $\Omega_c^{(r)}$, Ω_{xc} , V_x , $V_c^{(r)}$, and V_{xc} for electron densities of 10^{26} , 10^{24} , 10^{22} , and $10^{18}/\text{cm}^3$ for temperatures ranging from $t = 0.1$ –10. In the numerical evaluation, several features were noted. (a) It is found that the $l=0$ term in the series [Eq. (7)] alone produces the Debye-limit for $V_c^{(r)}$ when the $Q \rightarrow 0$ approximation is used for the corresponding polarizability for asymptotically large t . Thus

$$-V(Q) \chi(Q, l=0) \rightarrow \xi_D^2/Q^2,$$

where $k_F^2 \xi_D^2 = 4\pi n e^2 / k_B T$, so that from Eq. (7) upon a simple integration, we obtain

$$V_c^{(r)} \xrightarrow[t \rightarrow \infty, Q \rightarrow 0]{} -\frac{\pi^{1/2} e^3 n^{1/2}}{(k_B T)^{1/2}}. \quad (9a)$$

This result could be derived from the corresponding approximation for $\Omega_c^{(r)}$ with the same procedure:

$$\frac{\Omega_c^{(r)}}{V_0} \xrightarrow[t \rightarrow \infty, Q \rightarrow 0]{} -\frac{2}{3} \pi^{1/2} \frac{e^3 n^{3/2}}{(k_B T)^{1/2}}. \quad (9b)$$

(b) All other terms containing $l \neq 0$ in the series vanish faster than (9a) or (9b) for $t \rightarrow \infty$; only a few terms contribute significantly to the sums for high and intermediate values of t , beyond, for example, $t=3$. The sum $\sum_{l=1}^{\infty}$ converges rather poorly for small t ($t \lesssim 0.5$); the $l=0$ term is not as major a term as for large t , indicating that the dynamical part plays a dominant role for small t and low densities. (c) The computation of $\chi(Q, \nu_l)$ for $l \neq 0$ involves no singularities for any Q , a decided advantage not shared by the function when ν_l is a real continuous variable. The latter enters in an integral version of the results, viz., Eqs. (3) and (7). (d) In the numerical evaluation of the Q integrals in Eqs. (3) and (7), the upper limit of Q is chosen to be a suitable Q_{\max} , so that contributions from beyond this value are negligible. As t increases, the Q_{\max} values increase and the contributions from the intermediate and large Q values are quite significant. Even at a high density, for example, $n=10^{26} \text{ cm}^{-3}$, the result obtained from the Gell-Mann-Brueckner approxima-

TABLE I. Values of the exchange-correlation potential V_{xc} and the thermodynamic potential Ω_{xc} as a function of t for several electron densities. Correlation and exchange contributions are also tabulated. (All units in Rydbergs).

(a)							(c)						
$n=10^{26} \text{ cm}^{-3}$ ($T_F=9.1 \times 10^6 \text{ K}$)							$n=10^{22} \text{ cm}^{-3}$ ($T_F=2.0 \times 10^4 \text{ K}$)						
t	$-V_c^{(r)}$	$-V_x$	$-V_{xc}$	$-\Omega_c^{(r)}/N$	$-\Omega_x/N$	$-\Omega_{xc}/N$	t	$-V_c^{(r)}$	$-V_x$	$-V_{xc}$	$-\Omega_c^{(r)}/N$	$-\Omega_x/N$	$-\Omega_{xc}/N$
0.1	0.281	4.794	5.075	0.350	3.479	3.829	0.1	0.093	0.223	0.316	0.086	0.162	0.248
0.3	0.532	4.475	5.007	0.704	2.812	3.516	0.3	0.105	0.208	0.313	0.111	0.131	0.242
0.6	0.959	3.488	4.447	0.976	1.988	2.964	0.6	0.141	0.162	0.303	0.141	0.092	0.233
1.0	1.229	2.574	3.803	1.054	1.386	2.440	1.0	0.175	0.120	0.295	0.158	0.064	0.222
1.5	1.308	1.843	3.151	1.022	0.987	2.009	1.5	0.194	0.086	0.280	0.162	0.046	0.208
2.0	1.291	1.480	2.771	0.963	0.762	1.725	2.0	0.1996	0.069	0.269	0.159	0.035	0.194
2.5	1.246	1.214	2.460	0.905	0.620	1.525	2.5	0.2001	0.056	0.256	0.155	0.029	0.184
3.0	1.194	1.084	2.278	0.853	0.541	1.394	3.0	0.198	0.050	0.248	0.150	0.025	0.175
3.5	1.144	0.924	2.068	0.807	0.464	1.271	3.5	0.194	0.043	0.237	0.144	0.022	0.166
4.0	1.097	0.806	1.903	0.767	0.403	1.170	4.0	0.190	0.037	0.227	0.140	0.019	0.159
4.5	1.054	0.717	1.771	0.732	0.358	1.090	4.5	0.186	0.033	0.219	0.135	0.017	0.152
5.0	1.014	0.645	1.659	0.701	0.323	1.024	5.0	0.181	0.030	0.211	0.131	0.015	0.146
10.0	0.792	0.323	1.115	0.530	0.161	0.691	10.0	0.161	0.015	0.176	0.108	0.008	0.116
(b)							(d)						
$n=10^{24} \text{ cm}^{-3}$ ($T_F=4.2 \times 10^5 \text{ K}$)							$n=10^{18} \text{ cm}^{-3}$ ($T_F=42.3 \text{ K}$)						
t	$-V_c^{(r)}$	$-V_x$	$-V_{xc}$	$-\Omega_c^{(r)}/N$	$-\Omega_x/N$	$-\Omega_{xc}/N$	t	$-V_c^{(r)}$	$-V_x$	$-V_{xc}$	$-\Omega_c^{(r)}/N$	$-\Omega_x/N$	$-\Omega_{xc}/N$
0.1	0.169	1.033	1.202	0.177	0.750	0.927	0.1	0.0176	0.0103	0.0279	0.0148	0.0075	0.0223
0.3	0.236	0.964	1.200	0.288	0.606	0.894	0.3	0.0177	0.0096	0.0273	0.0152	0.0061	0.0213
0.6	0.382	0.751	1.133	0.390	0.428	0.818	0.6	0.0185	0.0075	0.0260	0.0161	0.0043	0.0204
1.0	0.488	0.555	1.043	0.429	0.299	0.728	1.0	0.0195	0.0055	0.0250	0.0169	0.0030	0.0199
1.5	0.531	0.397	0.928	0.426	0.213	0.639	1.5	0.0204	0.0040	0.0244	0.0174	0.0021	0.0195
2.0	0.534	0.319	0.853	0.408	0.164	0.572	2.0	0.0210	0.0032	0.0242	0.0178	0.0016	0.0194
2.5	0.523	0.262	0.785	0.388	0.134	0.522	2.5	0.0215	0.0026	0.0241	0.0179	0.0013	0.0192
3.0	0.507	0.234	0.741	0.369	0.117	0.486	3.0	0.0218	0.0023	0.0241	0.0180	0.0012	0.0192
3.5	0.490	0.199	0.689	0.352	0.100	0.452	3.5	0.0221	0.0020	0.0241	0.0180	0.0010	0.0192
4.0	0.473	0.174	0.647	0.337	0.087	0.424	4.0	0.0223	0.0017	0.0240	0.0180	0.0009	0.0190
4.5	0.461	0.154	0.615	0.323	0.077	0.400	4.5	0.0224	0.0015	0.0239	0.0179	0.0008	0.0187
5.0	0.443	0.139	0.582	0.311	0.070	0.381	5.0	0.0223	0.0014	0.0237	0.0178	0.0007	0.0185
10.0	0.365	0.070	0.435	0.240	0.035	0.275	10.0	0.0223	0.0007	0.0230	0.0176	0.0003	0.0179

tion⁵ involving the $Q \rightarrow 0$ limit at $t = 0$ accounts only for 50% of the full value of the "ring" sum. Our results for V_{xc} and Ω_{xc} agree very well with those of von Barth and Hedin⁸ at $t = 0$ in the metallic density region ($n \sim 10^{23} - 10^{24} / \text{cm}^3$) considered by them. This is a useful check. The corresponding high-temperature result of DeWitt¹⁰ for $\Omega_c^{(r)}$ ($t \rightarrow \infty$) served as a useful check on our results for both $\Omega_c^{(r)}$ and $V_c^{(r)}$.

From the Tables I(a)–I(d), the variation of the correlation potential as a function of t for various densities can be seen. In sharp contrast to the exchange potential V_x , $V_c^{(r)}$ is found to increase with t for all densities, go through a broad minimum, and then decrease very slowly with increasing t . In the intermediate degeneracy region, $0.3 < t < 3.5$, $V_c^{(r)}$ is substantially different from both the $t = 0$ and the $t \rightarrow \infty$ limits, typically merging with the Debye limit beyond $t \approx 10$. The minimum of $V_c^{(r)}$ shifts to lower values of t as the density

increases. The correlation enhancement is found to be more pronounced for high densities; for $n = 10^{26} / \text{cm}^3$, $V_c^{\text{min}}/V_c(t=0)$ is about 5 dropping to 2 for $n = 10^{18} / \text{cm}^3$. However, the decay rate of $V_c^{(r)}$ with t is much smaller for low densities. A similar trend is shared by $\Omega_c^{(r)}$.

Figure 1 exhibits the relative importance of V_x and $V_c^{(r)}$ for different n and t . V_x decreases rapidly through the intermediate degeneracy region and so it crosses over its $V_c^{(r)}$ counterpart at $t = t_0$ for a given density. This feature of correlation contribution dominating over the exchange is of increasing importance for all $t > t_0$. The locus of t_0 as a function of n distinguishing the two regions $V_c^{(r)} \geq V_x$ (as well as $\Omega_c^{(r)} \geq \Omega_x$) is given in Fig. 2. From this it is evident that at smaller densities, correlation is seen to be more important than exchange over practically the entire temperature range. The same general behavior is found for Ω_x and $\Omega_c^{(r)}$.

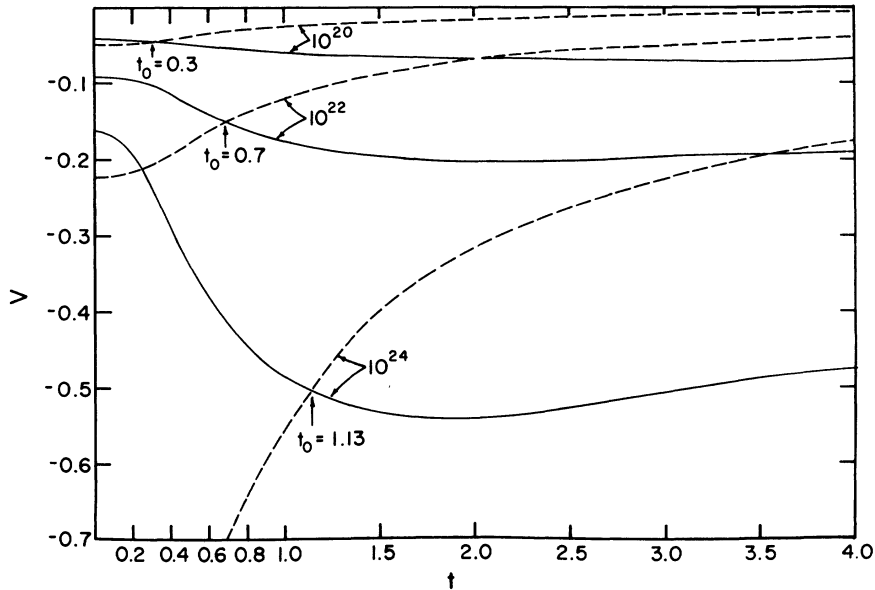


FIG. 1. The correlation potential $V_c^{(r)}[n, T]$ (solid curves) and the corresponding exchange potential $V_x[n, T]$ (broken curves) as a function of $t = T/T_F$ for three different densities (cm^{-3}). The arrows indicate the values t_0 where $V_c^{(r)}$ overtakes V_x . (Units in Rydbergs.)

A plot of V_{xc} vs t for different densities along with a plot of V_x vs t in Fig. 3 exhibits the importance of the use of V_{xc} in comparison to V_x alone. For high densities and small t values, V_{xc} is dominated by V_x (V_x is 84% of V_{xc} for $n = 10^{24} \text{ cm}^{-3}$ at $t = 0$) but for every n as t increases, V_x diminishes in its effects rapidly. Neglect of correlation thus would lead to significant errors in a wide range of n - T domain.

In Fig. 4 we show a plot of $V_{xc}[n, T]/V_{xc}[n, 0]$ vs n for $T = 1, 10, \text{ and } 100 \text{ eV}$. This shows that as the temperature is lowered over the density range of $10^{26} - 10^{18} \text{ cm}^{-3}$, the variation of V_{xc} for different temperatures has the same structure, like that of an inverted S curve. For a fixed high temperature, e.g., $T = 100 \text{ eV}$, the variation of this ratio drops

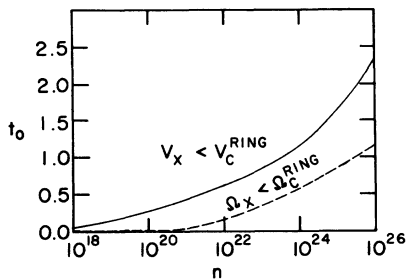


FIG. 2. The cross-over temperature $t_0 = T_0/T_F$ as a function of electron density $n (\text{cm}^{-3})$. $|V_c^{(r)}| > |V_x|$ above the solid curve while $|V_x| > |V_c^{(r)}|$ below it. The dotted curve distinguishes the corresponding regions for $|\Omega_c^{(r)}|$ and $|\Omega_x|$.

precipitously becoming much slower even at $T = 1 \text{ eV}$. This figure also shows the significance of the temperature effects on the exchange-corre-

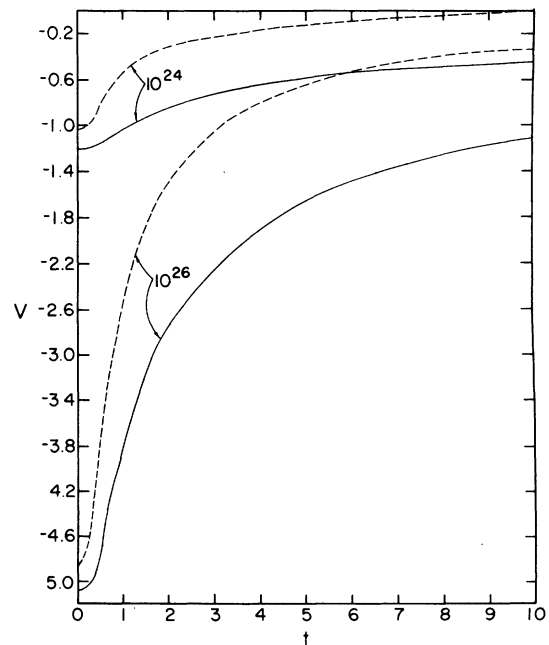


FIG. 3. The exchange-correlation potential $V_{xc}[n, T]$ (solid curves) along with the corresponding exchange contribution $V_x[n, T]$ (broken curves) as a function of $t = T/T_F$ for densities 10^{26} and 10^{24} cm^{-3} . The increased importance of correlation for intermediate and large t is evident.

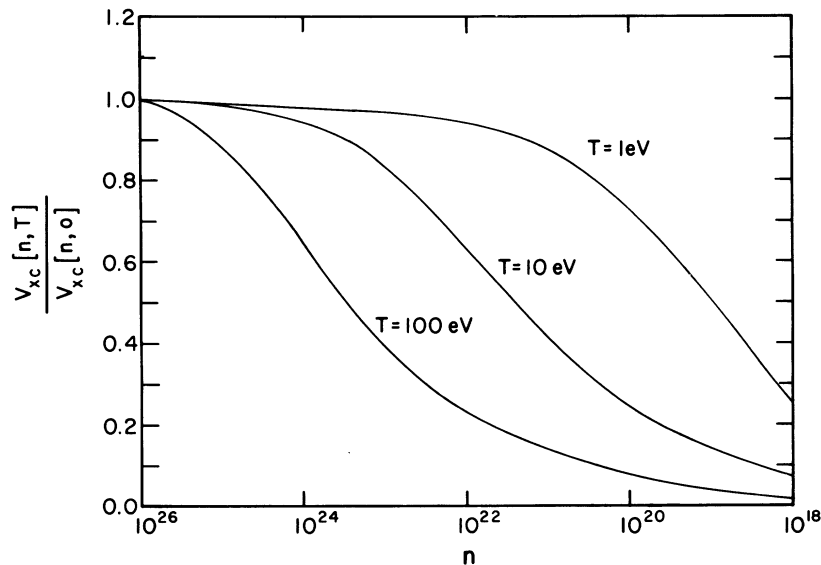


FIG. 4. $V_{xc}[n, T]$ scaled by the respective zero-temperature value $V_{xc}[n, 0]$ as a function of electron density $n(\text{cm}^{-3})$ at three different temperatures.

lation potential. The dependence of $\Omega_c^{(r)}/N$, Ω_x/N , and Ω_{xc}/N as a function of t and for various n values may be deduced from the tables. In the next section, we give a summary of the results obtained.

IV. SUMMARY

The exchange-correlation potential presented here represents an important step towards a complete development of the density-functional scheme for inhomogeneous electron systems

at nonzero temperatures. This work should prove useful in the work such as that of Rozsnyai² on atoms under unusual conditions as well as that of McMahan and Ross³ when the circumstance demands it ($t > 0.2$). The most important result emerging out of our investigation is that the correlation potential persists long after the exchange potential has vanished as a function of temperature. This is an expected result but the actual fall off had not been explored before. In this connection, Figs. 2 and 4 should be of special interest.

¹A. K. Rajagopal, *Adv. Chem. Phys.* **41**, 59 (1980).

²B. F. Rozsnyai, *Phys. Rev. A* **5**, 1137 (1972).

³A. K. McMahan and M. Ross, *Phys. Rev. B* **15**, 718 (1977).

⁴Uday Gupta and A. K. Rajagopal, *Phys. Rev. A* **21**, 2064 (1980).

⁵M. Gell-Mann and K. A. Brueckner, *Phys. Rev.* **106**, 364 (1957).

⁶G. Iwata, *Prog. Theor. Phys.* **24**, 1118 (1960).

⁷P. Nozières and D. Pines, *Phys. Rev.* **111**, 442 (1958).

⁸Ulf von Barth and L. Hedin, *J. Phys. C* **5**, 1629 (1972). We must mention here that L. Hedin and B. Lundqvist, [*ibid.* **4**, 2064 (1971)] were the first to give V_{xc} as a function of n at zero temperature. But for our pur-

poses, the work of von Barth and Hedin is more appropriate because they employ the ring-diagram approximation.

⁹E. W. Montroll and J. C. Ward, *Phys. Fluids* **1**, 55 (1958).

¹⁰H. DeWitt, *J. Math. Phys.* **3**, 1216 (1962).

¹¹W. D. Kraeft and W. Stolzmann, *Physica (Utrecht)* **97A**, 306 (1979).

¹²See, for example, A. L. Fetter and J. D. Walecka, *Quantum Theory of Many Particle Systems* (McGraw-Hill, New York, 1971). See, also, D. J. Thouless, *The Quantum Mechanics of Many-Body Systems*, (Academic, New York, 1972), 2nd ed.